NATIONAL ADVISORY COMMITTEE FOR AERONAUTICS

TECHNICAL NOTE 3584

FREE-CONVECTION EFFECTS ON HEAT TRANSFER FOR TURBULENT FLOW THROUGH A VERTICAL TUBE

By E. R. G. Eckert, Anthony J. Diaguila, and John N. B. Livingood

Lewis Flight Propulsion Laboratory
Cleveland, Ohio

Washington
December 1955

NATIONAL ADVISORY COMMITTEE FOR AERONAUTICS

TECHNICAL NOTE 3584

FREE-CONVECTION EFFECTS ON HEAT TRANSFER FOR TURBULENT FLOW THROUGH A VERTICAL TUBE

By E. R. G. Eckert, Anthony J. Diaguila, and John N. B. Livingood

SUMMARY

Experimental heat-transfer data for the turbulent flow of fluids through stationary vertical tubes with both small and large length-to-diameter ratios (to 40) are compared for the case where the acceleration of gravity is opposite in direction to the mean velocity in the tube and where the heat flows from the tube wall into the fluid. The division of the total flow region as characterized by the Grashof and Reynolds numbers into a forced-flow region, a free-flow region, and a mixed free- and forced-flow region is valid for both tubes. The limits of the different regions, originally established for a tube with small length-to-diameter ratio, apply on the basis of existing data to a tube with large length-to-diameter ratio.

INTRODUCTION

Experimental investigations of the free-convection effects on heat transfer for fluids flowing vertically through tubes with small and large length-to-diameter ratios were made by the NACA (ref. 1) and the Massachusetts Institute of Technology (ref. 2), respectively. The data from the two investigations were not analyzed on the same basis, however. In this report the M.I.T. data (large length-to-diameter-ratio tubes) are evaluated on the same basis as that used for the NACA data (small length-to-diameter-ratio tube).

An experimental investigation of the free-convection effects on heat transfer obtained for air flowing turbulently through a vertical tube is reported in reference 1. The experiments were conducted in a tube with a length-to-diameter ratio of 5; the tube surface was kept at constant temperature by a steam jacket and air flowed through the tube in either an upward or a downward direction. Free convection was created by gravity, so that the buoyancy forces in the heated layers near the tube wall were either parallel or opposite to the direction of the forced flow. The experiments were evaluated to obtain information on heat transfer in

that range of Reynolds and Grashof numbers in which the contributions of free and forced convection to the total heat flow are of the same order of magnitude. These results apply to flow through short tubes with free- and forced-convection forces acting either in the same or in opposite directions.

In reference 2 the results of experiments are reported in which Clark and Rohsenow at M.I.T. obtained heat-transfer data for distilled water flowing upward in a vertical nickel tube. The tube surface was electrically heated, and the portion of the tube where the data were obtained had a length-to-diameter ratio up to 40. Boiling, nonboiling, and burn-out conditions were investigated. Heat transfer at the nonboiling condition occurs under the influence of free- and forced-convection forces acting in parallel directions. These data can therefore be utilized to obtain correlations on heat transfer in the mixed free- and forced-convection range for tubes of larger length-to-diameter ratios. Such an analysis of the nonboiling data of reference 2 and a comparison with the results obtained in reference 1 is presented herein. Professor Rohsenow's help in suggesting this analysis and making it possible by releasing to the NACA the complete set of experimental results, including data on the tube wall and fluid bulk temperatures which are not contained in reference 2, is gratefully acknowledged.

Some measurements of heat-transfer coefficients in water and glycerine flowing in an upward direction through a vertical tube with a length-to-diameter ratio of 50 are reported in reference 3. The tube wall was heated externally by steam, and heat-transfer coefficients averaged over the tube length were obtained. The resultant plot of Nusselt number against Reynolds number based on diameter exhibits qualitatively the same trends as figure 14 of reference 1. No quantitative evaluation is possible, however, because the published data are insufficient for the calculation of the parameters used herein.

SYMBOLS

The following symbols, with consistent units, are used in this report:

C	constant
c_p	specific heat at constant pressure
D	tube diameter
G	mass velocity
Gr	Grashof number
Gr_x	Grashof number based on x and film temperature, $\frac{x^3\beta g(t_w - t_a)}{\nu_f^2}$

g	acceleration due to gravity
h	local heat-transfer coefficient
k	thermal conductivity
L	length of heated section of tube
Nu_d	Nusselt number based on diameter and bulk temperature, hD/k_b
Nu_x	Nusselt number based on x and film temperature, hx/k_f
Pr	Prandtl number based on film temperature, $c_{p,f}\mu_f/k_f$
$Pr_{b,f}$	Prandtl number defined by $c_{p,b}\mu_f/k_b$
Re	Reynolds number
Re_d	Reynolds number based on diameter and bulk temperature, GD/μ_b
Re_f	Reynolds number based on diameter and film temperature, GD/μ_f
Re_x	Reynolds number based on x and film temperature, Gx/μ_f
$Re_{x,w}$	Reynolds number based on x and wall temperature, Gx/μ_w
t	temperature
v	velocity
x	characteristic dimension measured from lower edge of heated section
β	coefficient of thermal expansion, $1/t$
μ	dynamic viscosity
ν	kinematic viscosity

Subscripts:

a	air at tube axis
b	bulk
d	diameter

f film

w wall

x location along tube in axial direction

M.I.T. INVESTIGATION

The M.I.T. investigation (ref. 2) was made primarily to obtain information on heat transfer to heated and pressurized water flowing through a tube under conditions of local boiling occurring on the tube walls. However, some runs were also made without boiling, and these will be used in the present investigation. A short description of the test setup and the significant results obtained is presented in this section.

3700

Discussion of Experiments

A sketch of the test section used in the M.I.T. investigation is shown in figure 1. The test section consisted of a nickel tube of 0.1805-inch inner diameter, 0.2101-inch outer diameter, and 9.4-inch length (over-all length-to-diameter ratio $L/D = 52$). Nonboiling data were recorded at stations along the tube for length-to-diameter ratios from 8.04 to 39.1. The tube was heated electrically by a current flowing through the tube wall in the axial direction. Inner tube wall temperatures at each of five stations along the tube were determined by measuring the outer-wall temperatures and calculating the temperature drop across the tube wall from the electric current and the tube properties and dimensions. The thermocouples were insulated from the tube wall by a sheet of mica 0.0015 inch thick. The bulk temperature of the water entering the test section was measured $5\frac{1}{2}$ inches upstream of the heated section; the exit temperature, 9 inches downstream of the heated section. A temperature drop in the heated water from the upstream measuring station to the entrance of the test section was discovered in runs in which the test section was not heated, and a corresponding correction was applied to obtain the water inlet temperature from the upstream temperature reading. The test section was insulated by 85-percent magnesia insulation to minimize heat losses to the atmosphere. The bulk temperature of the water at various stations along the tube was determined from the enthalpy increase of the water to the particular location, assuming the increase to be equal to the electric energy transformed into heat in the particular tube section. The mass velocity of the water was measured by orifices. The orifices were of 0.018-, 0.024-, and 0.042-inch diameter and were individually calibrated.

Heat-transfer data were obtained for inlet pressures of 500, 1500, and 2000 pounds per square inch absolute, for a range of inlet velocities from about 0.04 to 1.4 feet per second, and for inlet water temperatures from 94° to 510° F.

Results

The experimental results are presented in tabular form in table II of reference 2 together with the parameters

$$Nu_d = \frac{hD}{k_b}$$

$$Re_f = \frac{GD}{\mu_f}$$

$$Pr_{b,f} = \frac{c_{p,b}\mu_f}{k_b}$$

These parameters and their converted equivalents based on length and film temperature covered the following ranges:

$2.18 < Nu_d < 83.3$	$32.15 < Nu_x < 2223$
$478 < Re_f < 17,540$	$13,800 < Re_x < 628,700$
$0.65 < Pr_{b,f} < 1.94$	$0.77 < Pr < 1.94$
	$6.9 \times 10^7 < Gr_x < 8.6 \times 10^{11}$

The data are analyzed and discussed in reference 2. Figure 2 shows a typical wall-temperature distribution curve as the dashed line. The fact that this wall-temperature distribution resembles quite closely the linear variation of the fluid-temperature curve indicates that the film heat-transfer coefficient varies only slightly along the tube. The solid curves represent some unusual distributions obtained for velocities between 0.25 and 0.6 foot per second; these results could be duplicated, and the saw tooth could be shifted along the tube by altering the fluid velocity or the heat flux. In this velocity range, the Reynolds number based on diameter varied from 1650 to 4800, a range in which transition to turbulence is expected to occur. The investigators therefore explained this peculiar temperature field by assuming laminar flow upstream of the break in the curve and turbulent flow downstream of it.

Figure 3 shows a plot of the measured Nusselt number (hD/k_b) against the Reynolds number (Gx/μ_w) based on x with the Reynolds number (GD/μ_b) based on diameter as parameter. It can be seen that for most runs the

Nusselt number increases sharply in the range $60,000 < Re_x < 100,000$. This increase also was interpreted as an indication of transition, and it is assumed in reference 2 that this transition is excited by the effects of free convection in the vertical tube.

The effects of superimposed free convection are shown in figure 4. The Nusselt numbers in this figure are multiplied by the -0.2 power of the Prandtl number and by the 0.14 power of the ratio of viscosity based on wall and bulk temperatures $\left[\left(\frac{hD}{k_b}\right)Pr_{b,f}^{-0.2}\left(\frac{\mu_w}{\mu_b}\right)^{0.14}\right]$, assuming that the resulting parameter is independent of Prandtl number and of heating rate (ref. 4). The parameter in the brackets is plotted against the diameter Reynolds number GD/μ_b. Each individual line indicates the variation of this parameter along the tube length. For Reynolds numbers between 1000 and 3000, most of the data are considerably higher than the line through the data for larger Reynolds numbers. A few points are lower than the calculated Nusselt number of 4.36 for laminar forced flow through a tube with constant heating rate at the wall. These data points are probably in error.

3700

NACA INVESTIGATION

The NACA experiments (ref. 1) and their evaluation will be discussed briefly in this section to facilitate a comparison with the M.I.T. investigation. Only the experiments with free- and forced-convection forces acting in parallel direction will be included.

Discussion of Experiments

The test setup used in the NACA investigation is shown in figure 5. Because it was designed to study heat transfer by free and mixed convection in the turbulent range, the dimensions are large. The tube, made of mild steel, had an outer diameter of 24 inches and a length of $13\frac{1}{2}$ feet. The heated test section was 10 feet long ($L/D = 5$). Air was introduced through an inlet pipe B_b and passed through a dense screen E into the test section proper. It left this section through a second screen E and outlet pipe C_t. The tube test section was surrounded by an insulated jacket and steam heated. Sixteen condensate chambers were arranged along the heated section of the tube to collect and measure the condensate. Five thermocouples along the heated section were used to measure the wall temperatures. Air temperatures at various locations along the tube were measured with thermocouple probes. A more detailed description of the apparatus is given in reference 1.

Heat-transfer data were obtained for air entering the test section with a temperature of about 80° F and with pressures from atmospheric to 125 pounds per square inch absolute. Inlet-air velocities ranged from 1 to 10 feet per second.

Results

The heat-transfer data are presented in reference 1 by the parameters

$$Nu_x = \frac{hx}{k_f}$$

$$Re_d = \frac{GD}{\mu_b}$$

$$Re_x = \frac{Gx}{\mu_f}$$

$$Gr_x = \frac{x^3 \beta g (t_w - t_a)}{\nu_f^2}$$

These experiments covered the following ranges:

$$130 < Nu_x < 3500$$

$$36{,}000 < Re_d < 377{,}000$$

$$50{,}000 < Re_x < 700{,}000$$

$$1.4 \times 10^9 < Gr_x < 5.7 \times 10^{12}$$

Figures 6 to 8 show the results of the NACA investigation. Figure 6 presents the dimensionless parameters in the form in which they were obtained from the experiments. In this figure, the local Nussel number Nu_x is plotted against $Gr_x Pr$ with the Reynolds number Re_d as parameter. The difference between the tube wall temperature t_w and the air temperature t_a in the tube axis and at the particular distance x is used to evaluate the Grashof number. Figure 6 shows the results for three different inlet-air pressures. The figure does not lend itself to an interpretation of the data. Therefore, values from the curves (not actual data points) in figure 6, for specified values of Re_x, are replotted in figure 7. In both figures, they are indicated as solid points.

Points with equal Reynolds numbers Re_x are interconnected by solid lines in figure 7. Also inserted as a dashed line is a mean data line obtained in a special series of runs, called free-convection runs, in which the inlet and outlet (B_b and C_b, respectively) of the lower end of the tube were closed and in which cold air was maintained at the upper

tube end (air admitted through B_t and removed through D, C_t closed). The data in figure 7 can now be readily interpreted. The figure shows that, for large values of Gr_xPr, all constant Re_x curves converge into this dashed line (free-convection region). Conversely, each constant Re_x curve becomes more and more horizontal with decreasing values of Gr_xPr, indicating that the Nusselt number becomes independent of the Gr_xPr numbers in this region (forced-flow region). Figure 7 therefore establishes the limits between the forced-flow region in which free convection is negligible, the free-flow region where the free convection practically alone determines the heat transfer, and the mixed-flow region in which both free and forced convection are of equal importance. Limits between these regions can be established by determining a line on which forced-flow heat transfer is affected to a specified amount (10 percent) by free-convection effects (forced-convection limit line in fig. 7) and a line on which free-convection heat transfer is affected to 10 percent by superimposed forced flow. The latter limit is not indicated in figure 7; however, it is located slightly above the dashed line. All Re_x curves contain a noticeable dip, indicating that heat transfer is lower in the mixed-flow region than for forced flow at the same Re_x. A possible explanation for this effect is presented in reference 1.

Figure 8 presents the same data as figure 7, except that the abscissa and the parameter have been interchanged. The free- and forced-convection regions again may be recognized in this figure by the fact that all the curves tend to converge asymptotically into a single line for high Reynolds numbers and that all curves become horizontal for low Reynolds numbers. The correlation for a turbulent boundary layer along a flat plate (ref. 4, p. 117) is shown as a solid line, and two correlations for the turbulent intake region of a pipe as dashed lines. The lines for constant Gr_xPr tend to converge into the line for $x/D = 5$. For a more detailed discussion of this point, see reference 1.

EVALUATION AND COMPARISON OF M.I.T. AND NACA RESULTS

Conversion of Data

According to dimensional analysis, heat transfer connected with mixed forced- and free-convection flow through a circular tube is expected to depend on the following parameters:

Flow parameters: Re, Gr, Pr
Geometric parameters: x/D, L/D
Boundary conditions: Velocity and temperature field at entrance cross section, temperature distribution along tube wall, direction of vector quantities relative to each other, that is, direction of heat flow at surface, direction of velocity at entrance, direction of gravitational acceleration, direction of temperature gradient along tube wall

The number of parameters in a mixed-flow problem is, therefore, very large, and it is practically impossible to vary all of them in a reasonable research effort.

The NACA investigation was planned so as to obtain locally constant velocity and temperature in the entrance cross section and over the heated portion of the tube surfaces. In the group of experiments that will be discussed herein, the velocity at the entrance had a direction opposite to the gravitational acceleration, and the heat flow was from the wall towards the tube interior. In the evaluation of the tests, it was assumed that no L/D influence would be present and that the x/D influence would disappear when Re and Gr were based on the length x. Satisfactory correlation of the data was obtained on this basis.

The M.I.T. investigation differs from the NACA tests in some of the boundary conditions. The velocity enters the heated section with a developed profile; there exists a nearly uniform temperature gradient along the tube wall. The direction of heat flow, entrance velocity, and gravitational acceleration are the same as in the NACA study. There is little reason to expect an upstream influence of the tube exit on the flow through the tube interior as long as no recirculation within the tube occurs. Therefore, the influence of L/D on heat transfer in this tube configuration is probably negligible; however, there is less reason to assume that the influence of x/D can be eliminated by use of either x or D as the length parameter in Re and Gr, since the range of Re values is such that forced-flow heat transfer is known to depend on x/D in addition to Re. Nevertheless, the evaluation was tried on the basis of the parameters used in the NACA investigation. No influence of the other parameters was apparent in the correlations obtained in this way. However, some of the scatter of the test points may be attributed to this fact.

In order to compare the results of the two experiments and to determine the free-convection effects on heat transfer, the various parameters in the two reports must be converted to a uniform basis and the differences in the Prandtl numbers (water in the one case and air in the other) must be resolved. Data presented in reference 2 were not sufficient for the calculation of the Grashof number and therefore Professor Rohsenow kindly forwarded the required data (values of the wall temperature and the fluid bulk temperature) to the NACA.

From this information, the Grashof numbers were calculated, the Nusselt numbers listed in table II of reference 2 were converted to the film-temperature basis and the local distance x, and the corresponding Prandtl numbers were converted to the film-temperature basis. The Grashof number calculated from the M.I.T. experiments is based on the difference between wall and bulk temperature. It is not exactly comparable with the Grashof number in the NACA report (ref. 1); this number is based on the difference between the wall temperature and the fluid temperature in the

tube axis. It is believed that the effect of this difference is small. Another difficulty is connected with the fact that the two sets of experiments were made at different Prandtl numbers. This difficulty was resolved in the following way.

It has been established that in a Prandtl number range which is not too large free convection depends on the product Gr_xPr. There is some indication that this holds for turbulent flow as well as for laminar flow (ref. 5). An established relation for turbulent flow through a tube is

$$Nu_d = CRe_d^{0.8}Pr^{0.4} = C\left(Re_dPr^{1/2}\right)^{0.8} \tag{1}$$

$$Nu_x = C\left(\frac{x}{D}\right)^{0.2}\left(Re_xPr^{1/2}\right)^{0.8}$$

Therefore, a parameter $Re_xPr^{1/2}$ was used to bring both tests to the same basis.

Presentation and Discussion of Data

The combined data of the two investigations are plotted in figures 9 and 10. Figure 9 presents Nu_x plotted against Gr_xPr for various values of the parameter $Re_x\sqrt{Pr}$. The solid curves represent the NACA data, and were obtained from figure 7 by the incorporation of $\sqrt{Pr}$ in the parameter. From the data contained in the M.I.T. report, points were selected for which the parameter $Re_x\sqrt{Pr}$ agreed within a specified range with the values used for the presentation of the NACA results. The M.I.T. values are indicated by the points in figure 9. Mean lines are drawn through the points as dash-dot lines. The dashed line is the mean data line for free-convection flow taken from figure 7. The solid symbols and the connecting line will be explained later.

The dash-dot curves in figure 9 represent the results of the experiments for length-to-diameter ratios from 8 to 40. No effect of length-to-diameter ratio is apparent. The curves exhibit essentially the same behavior as the solid lines interpreting the tests for the small length-to-diameter ratios (up to 5). They also tend to converge into a single line for large values of the parameter Gr_xPr and tend to become horizontal for low values of this parameter, indicating that in this latter range free convection has a negligible effect on heat transfer. There is also some indication in the tests at larger values of the parameter $Re_x\sqrt{Pr}$ in the mixed-flow region that heat-transfer coefficients are somewhat lower than in the forced- and in the free-convection regions at the same value of $Re_x\sqrt{Pr}$. Such a dip is also observed on the solid lines, representing results obtained in the tube with small length-to-diameter

ratio. It should be noted that in reference 1, McAdams rule (ref. 5, p. 250) was recommended for the calculation of heat-transfer coefficients in the mixed-flow region. This rule states that, for this region, coefficients can be calculated from both forced-flow and free-flow relations, and the larger coefficient should be used. Such calculated coefficients will be somewhat too large according to the experimental results shown in figures 7 and 9. Since the knowledge of heat transfer in the mixed-flow region is limited because of considerable scatter of the test points, it appears logical to recommend the use of McAdams' rule to flow through tubes with length-to-diameter ratios up to about 40 for the calculation of heat-transfer coefficients in the mixed-flow region.

Within the accuracy with which a prediction can be made, it appears also that the limits between the forced-flow, the mixed-flow, and the free-flow regions, which were established in reference 1, can be tentatively used for flow through tubes with length-to-diameter ratios up to 40. The limit between forced and mixed flow (ref. 1) is

$$Re_x = 8.25\ (Gr_x Pr)^{0.40}$$

and the limit between mixed and free flow (ref. 1) is

$$Re_x = 15\ (Gr_x Pr)^{0.40}$$

Heat-transfer coefficients measured for the tube with large length-to-diameter ratios in the flow range which is apparently free convection are somewhat lower than the values found for the tube with small length-to-diameter ratio, and indicated in figure 9 by the dashed line. No explanation for this fact is apparent at present. It is not believed that it is due to the larger over-all length-to-diameter ratio, as will be explained later.

It is of interest to check how the sudden increase in Nusselt number discussed with regard to figure 3 appears in figure 9. For this purpose, five points have been numbered in both figures. It can be recognized that the increase in Nusselt numbers that causes the break in the lines of figure 3 also appears in figure 9; however, it is not as pronounced. From figure 9 it can be seen that the situations that cause such a break and irregular wall-temperature distribution are in a range where free-convection effects are dominant.

Figure 10 is essentially a cross plot of figure 9. The roles of the abscissa and the parameter are now interchanged. The solid curves are taken from figure 8 and therefore represent the data for constant values of $Gr_x Pr$. Again, data points are selected from reference 2 for which the parameter $Re_x/\sqrt{Pr}$ agrees within a specified range with the values for which the solid curves in figure 10 were drawn. These points are inserted in the figure.

It is to be expected that the points for a fixed value of the parameter Gr_xPr converge for large values of the parameter $Re_x/\sqrt{Pr}$ into established forced-flow relations describing heat transfer in a tube with large length-to-diameter ratio. To show how well this situation is fulfilled, two curves have been added to figure 10 as dashed lines which represent heat transfer in a tube with length-to-diameter ratios of 8.04 and 39.1. These curves have been obtained in the following way: It is assumed that heat transfer in the forced-flow region, and for the length-to-diameter ratios in question, is described by the following relation, developed by L. M. K. Boelter, (ref. 4, p. 115):

$$Nu_d = 0.0243\ Re_d^{0.8}\ Pr^{0.4} \tag{1}$$

In figure 10, Nusselt and Reynolds parameters are used that are based on the length x measured along the tube instead of the diameter D, which is the length parameter in equation (1). Changing to the Nusselt and Reynolds number based on x instead of on D results in the following equation:

$$Nu_x = 0.0243\left(\frac{x}{D}\right)^{0.2} Re_x^{0.8}\ Pr^{0.4} \tag{2}$$

The tests by Clark and Rohsenow determined heat-transfer coefficients at stations for which the length-to-diameter ratio varied between 8.04 and 39.1. In order to determine what the corresponding limiting values for the Nusselt number based on the length x were, equation (2) has been solved for these two length-to-diameter ratios; the corresponding lines are the dashed lines in figure 10. Hausen's equation (used in ref. 1) gives practically the same result. It should therefore be expected that the experimental points for large Reynolds numbers converge into the range limited by these two lines. Actually, the test points appear to lie somewhat lower. Equation (1), for the heat-transfer coefficient based on diameter, has also been inserted as the dashed line into figure 4. It can be seen also in this figure that heat-transfer coefficients measured in the range that is expected to be the forced-flow range are lower than the established forced-flow relations. This then parallels the behavior of the test data in the free-flow region in which the experimental points according to figure 9 are also lower than expected from the results obtained on tubes with small length-to-diameter ratios.

The following question is obvious in connection with the presentation of figures 9 and 10: Would it have been better to base the dimensionless parameters used in these figures on the diameter rather than on the distance x, because it must be expected that, for long tubes, the diameter is the main length parameter influencing heat transfer and flow? For the free-flow region, the following statement can be made. If a relation exists between Nusselt number and the product of Grashof and Prandtl numbers of the form

$$Nu = C(GrPr)^{1/3}$$

then the heat-transfer coefficient is independent of the length parameter and Nusselt and Grashof numbers may be based on either x or D (ref. 5, p. 172). The dashed line in figure 9 corresponds to an exponent which is nearly 1/3. On the other hand, a plot of the form of figure 9 that would use D instead of x would crowd all test points very closely together, and it would be very difficult to interpret the test results in such a diagram. The same reasoning led to the use of the dimensionless parameters based on x in figure 10.

CONCLUSIONS

The following conclusions can be reached from the comparison of the experiments on heat transfer through tubes with both small and large length-to-diameter ratios for the case where the body force is opposite to the acceleration of gravity and the heat flows from the wall to the fluid:

1. Experiments in tubes at small (up to 5) and large (8 to 40) length-to-diameter ratios, when correlated on the basis of Reynolds and Grashof parameters, exhibit qualitatively the same behavior in the forced-, mixed-, and free-convection regions.

2. The limits between the forced-flow region, the mixed-flow region, and the free-flow region which were established at the Lewis laboratory for a length-to-diameter ratio up to 5 can be used for a length-to-diameter ratio up to about 40 on the basis of existing data. It must be expected that these limits are influenced to a certain degree by the length-to-diameter ratio; however, the accuracy of the tests is not sufficient to establish this effect.

3. For the condition which has been investigated, namely, forced-flow forces acting opposite to the gravitational acceleration and heat flow from the wall to the fluid, heat-transfer coefficients have been measured that are lower in the mixed-flow region than either in the forced- or in the free-convection region for the same value of the parameter $Re_x/\sqrt{Pr}$ (where Re_x is Reynolds number at a distance x along the tube wall and Pr is Prandtl number) for flow through tubes with both small and large length-to-diameter ratios.

4. McAdams' rule, which suggests for the mixed-flow region the use of the larger heat-transfer coefficient obtained from forced- and free-convection correlations, is recommended on the basis of existing information for flow through tubes with length-to-diameter ratios up to about

40. This procedure should give heat-transfer coefficients in the mixed-flow region which are somewhat too large, according to the third conclusion.

Lewis Flight Propulsion Laboratory
National Advisory Committee for Aeronautics
Cleveland, Ohio, September 15, 1955

REFERENCES

1. Eckert, E. R. G., Diaguila, Anthony J., and Curren, Arthur N.: Experiments on Mixed-Free- and -Forced-Convective Heat Transfer Connected with Turbulent Flow Through a Short Tube. NACA TN 2974, 1953.

2. Clark, John A., and Rohsenow, Warren M.: Local Boiling Heat Transfer to Water at Low Reynolds Numbers and High Pressure. Div. Ind. Cooperation, M.I.T., July 1, 1952. (For Office Naval Res., Contract N5ori-07827; NR-035-267; D.I.C. Proj. No. 6627.) (See also Trans. A.S.M.E., vol. 76, no. 4, May 1954, pp. 553-562.)

3. Wetjen, K. A.: Wärmeübergang bei strömenden Flüssigkeiten im senkrechten Rohr mit und ohne Eigenkonvektion. Chem.-Ing. Tech., Bd. 26, 1954, pp. 454-460.

4. Eckert, E. R. G.: Introduction to the Transfer of Heat and Mass. McGraw-Hill Book Co., Inc., 1950.

5. McAdams, William H.: Heat Transmission. Third ed., McGraw-Hill Book Co., Inc., 1954.

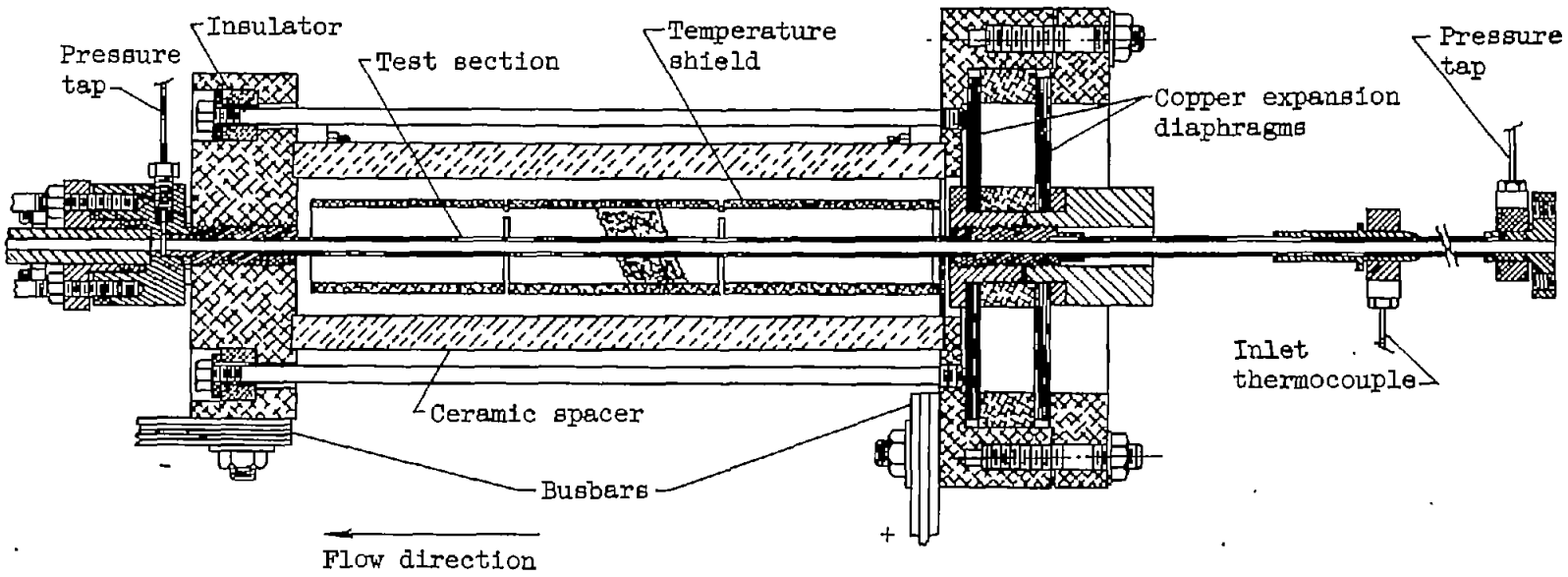

Figure 1. - Test section of apparatus used in M.I.T. investigation. (Obtained from ref. 2.)

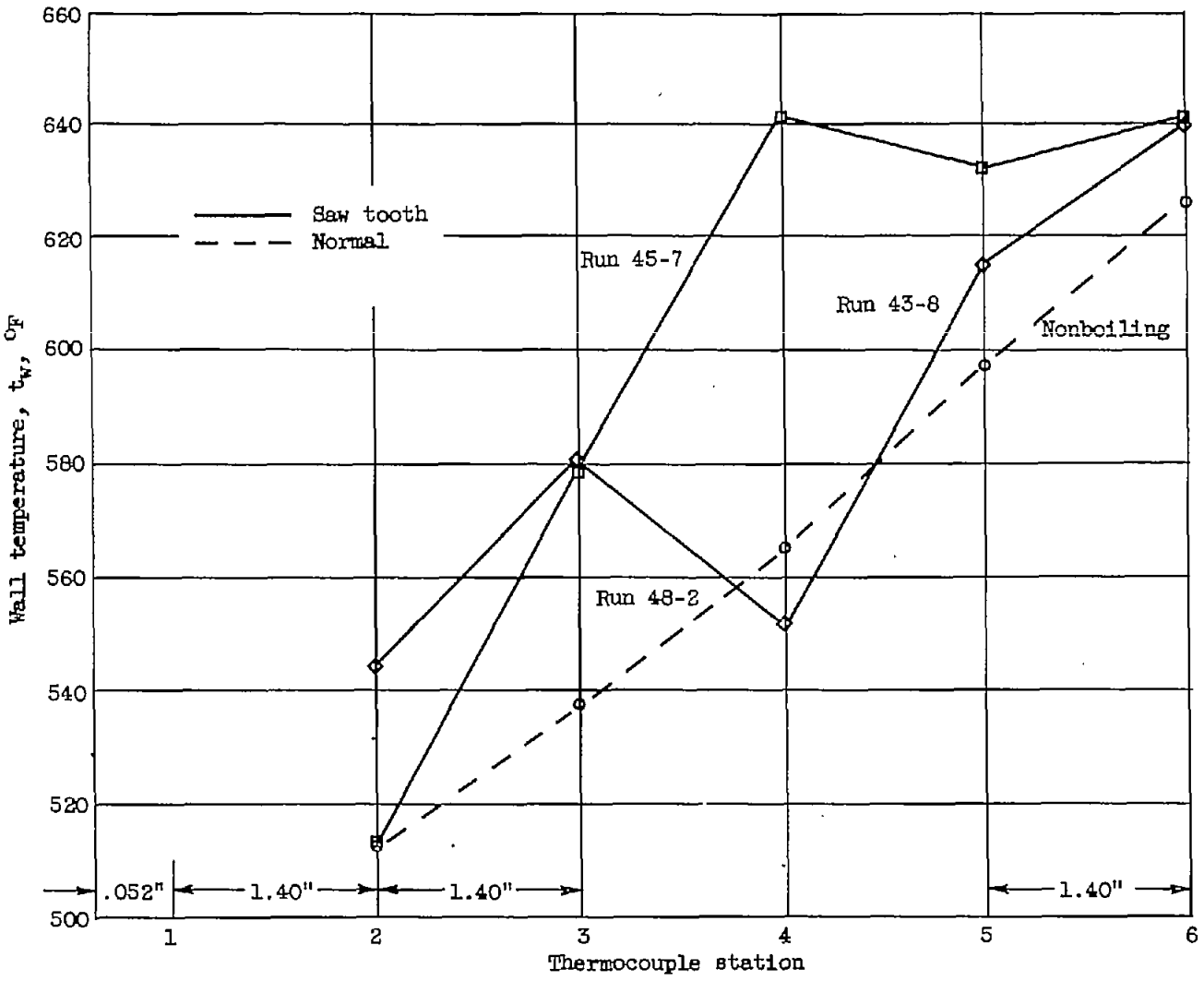

Figure 2. - Wall-temperature distributions obtained in test section of figure 1. (Obtained from ref. 2.)

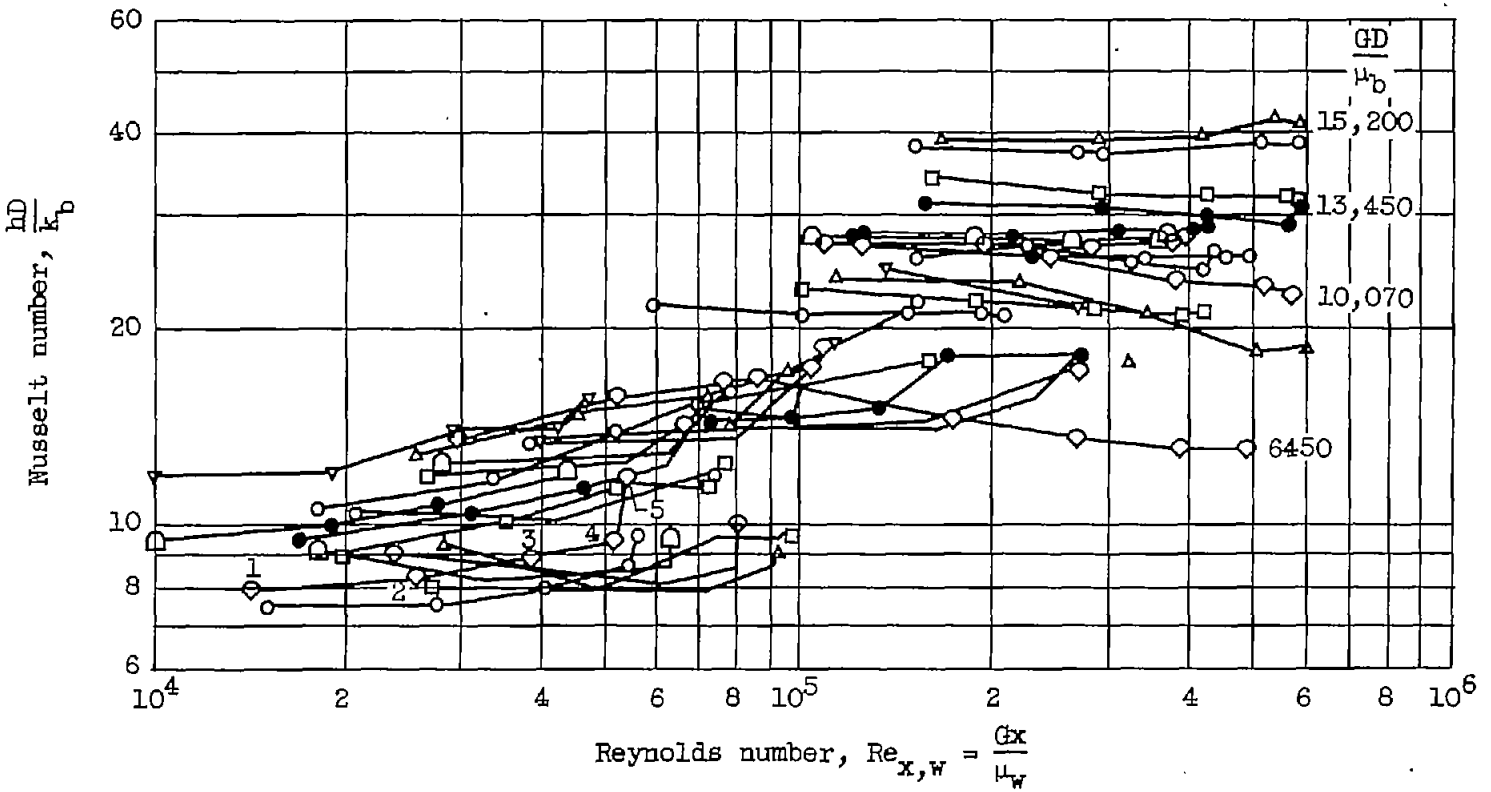

Figure 3. - Correlation of heat-transfer data for tube with large length-to-diameter ratio plotted over the Reynolds number based on characteristic dimension. (Obtained from ref. 2.)

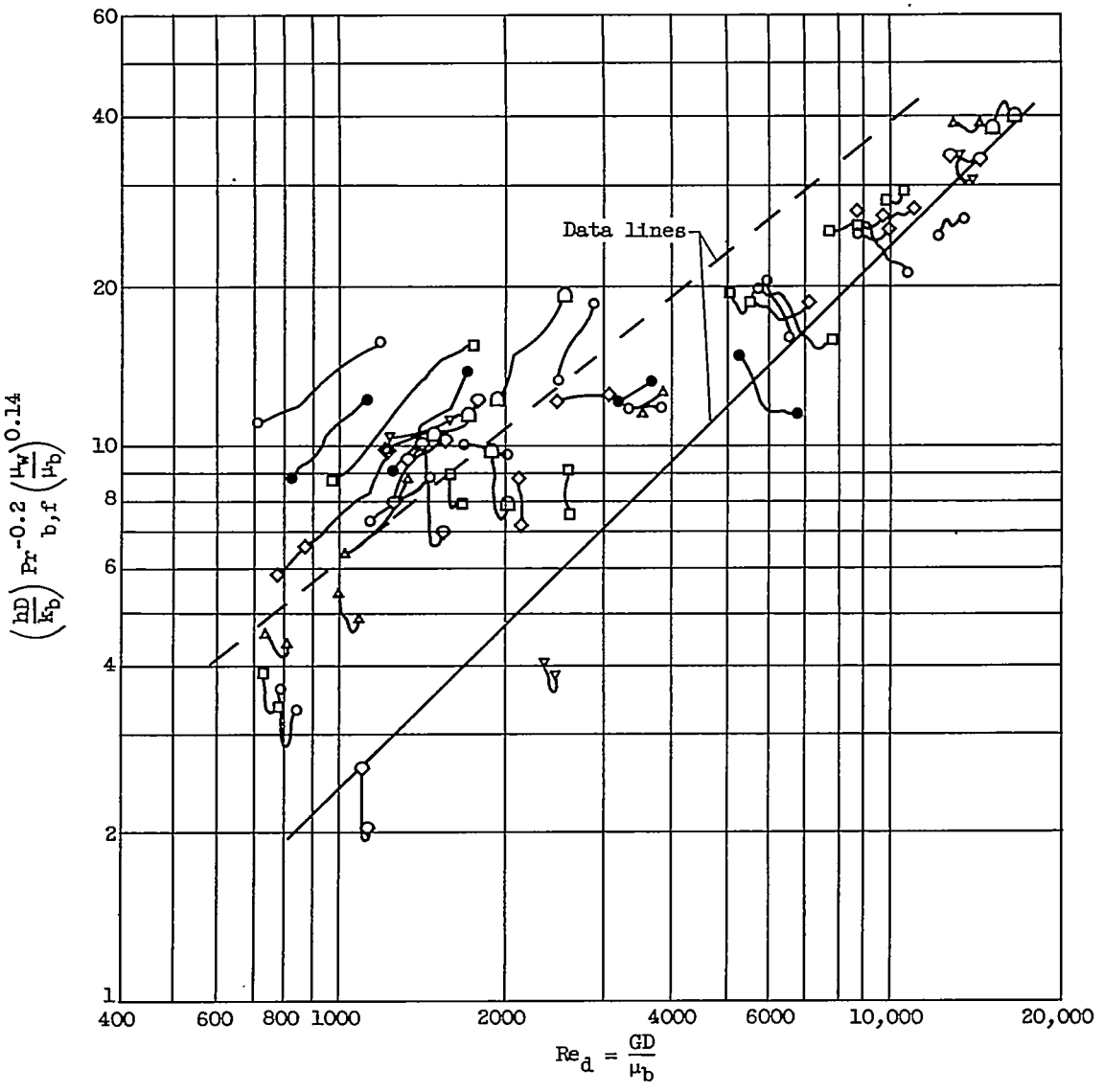

Figure 4. - Correlation of heat-transfer data for tube with large length-to-diameter ratio showing effects of free convection. (Obtained from ref. 2.)

3700

CS-3 back

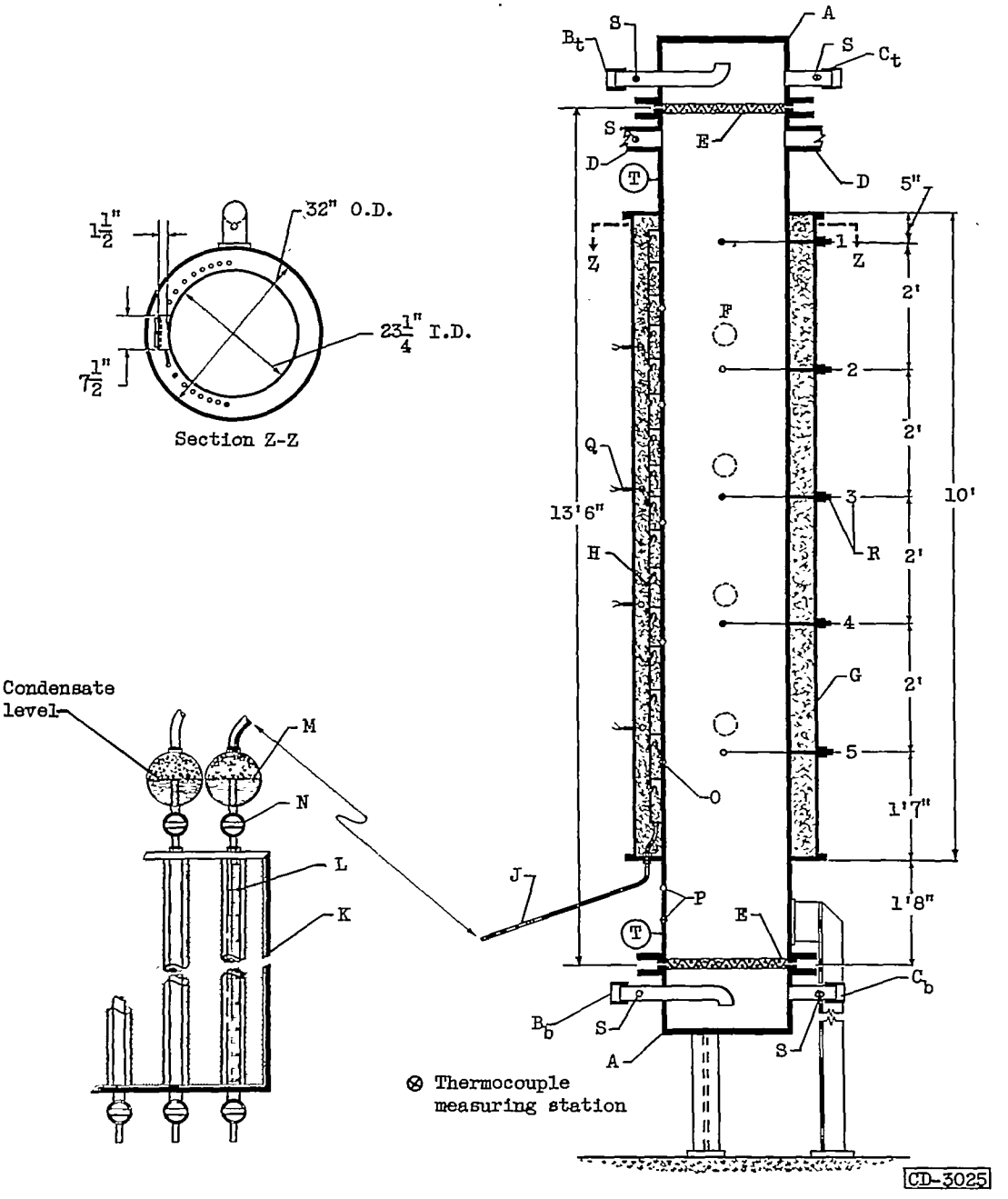

A Top and bottom covers
B_b Inlet-line bottom cover
B_t Inlet-line top cover
C_b Exhaust-line bottom cover
C_t Exhaust-line top cover
D Exhaust line on tube
E Screening
F Inlets to steam jacket
G Steam jacket
H Condensate chambers
J Condensate lines (exposed)
K Burette board
L Burette
M Condensate collector
N Petcock
O Heated-wall thermocouple
P Unheated-wall thermocouple
Q Steam thermocouple
R Probes
S Inlet- and exhaust-air thermocouples
T Air pressure taps

Figure 5. - Test section of apparatus used in NACA investigation (ref. 1).

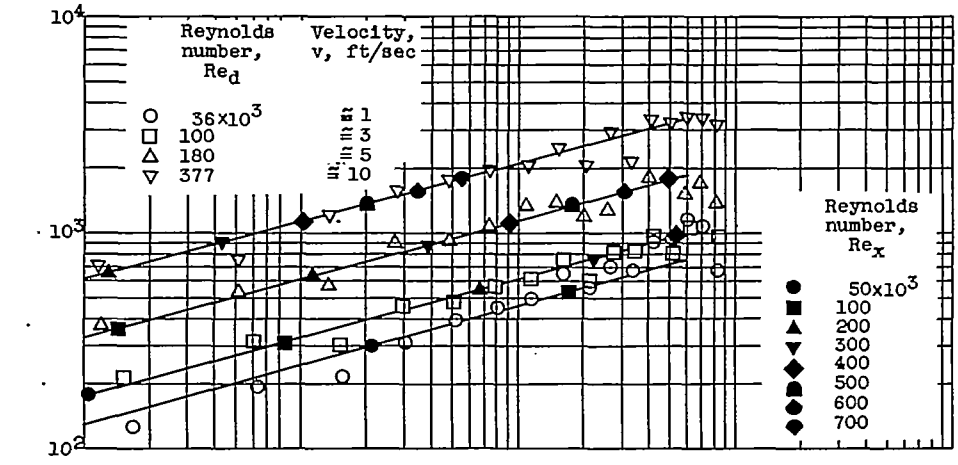

(a) Air pressure, 44.3 pounds per square inch absolute.

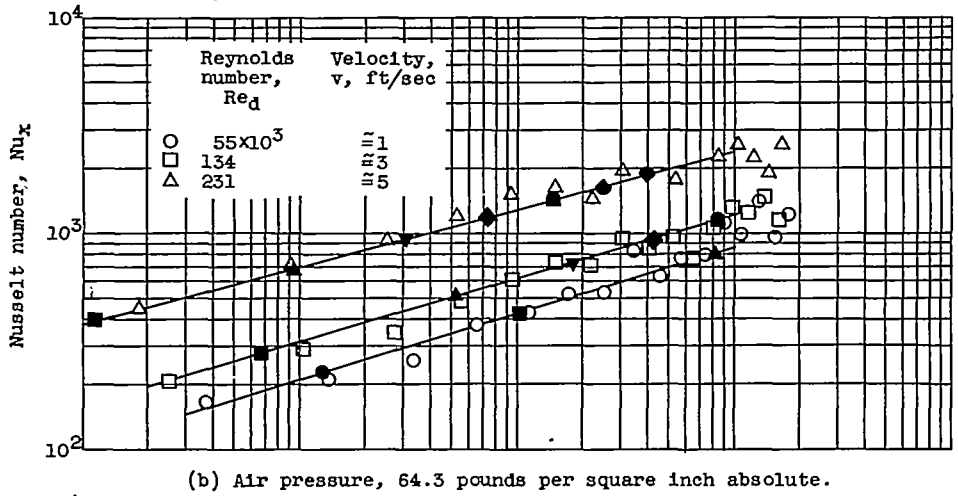

(b) Air pressure, 64.3 pounds per square inch absolute.

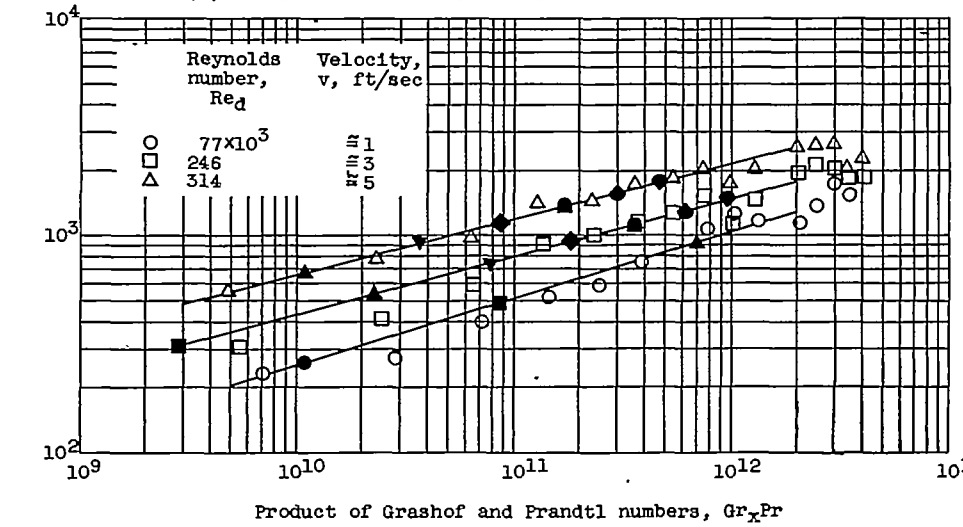

(c) Air pressure, 99.3 pounds per square inch absolute.

Figure 6. - Correlation of heat-transfer data for turbulent flow obtained in tube with small length-to-diameter ratio (ref. 1).

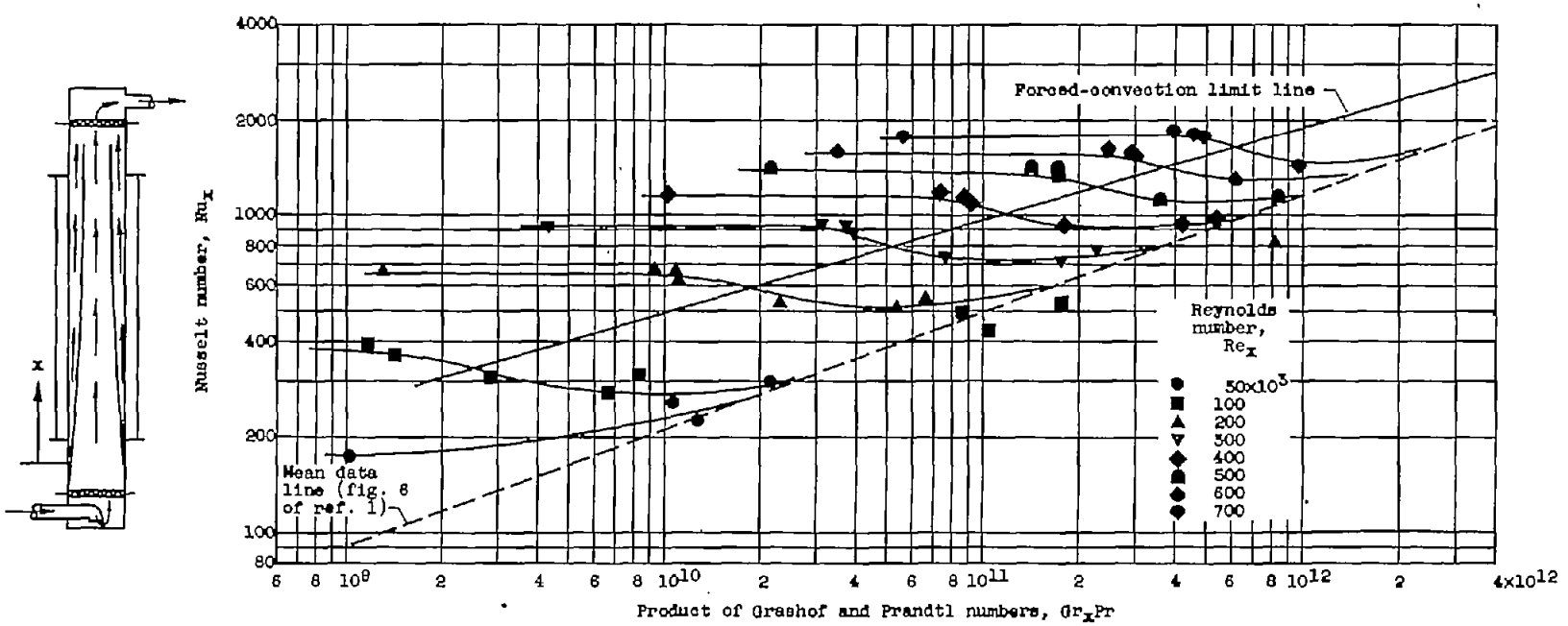

Figure 7. - Effects of free convection from correlation of heat-transfer data for turbulent flow in tube with small length-to-diameter ratio (ref. 1).

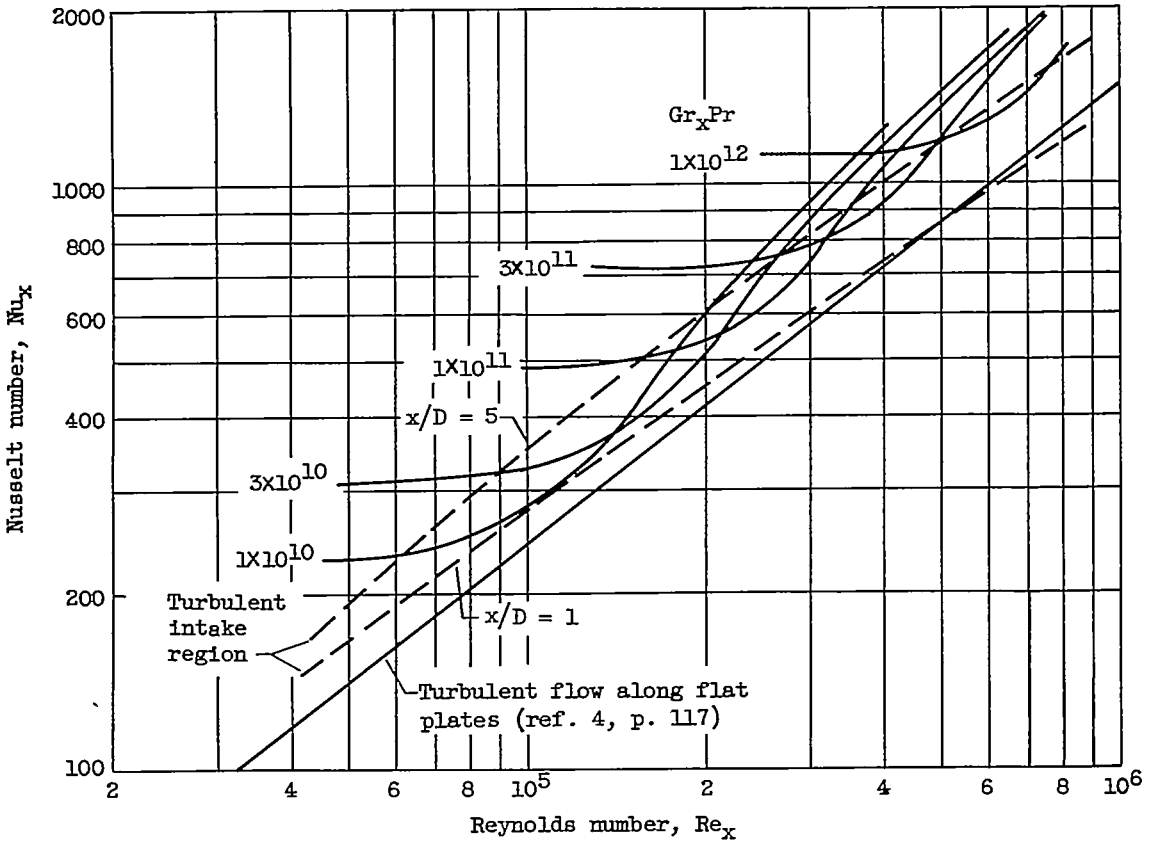

Figure 8. - Effects of forced convection from correlation of heat-transfer data for turbulent flow in tube with small length-to-diameter ratio (ref. 1).

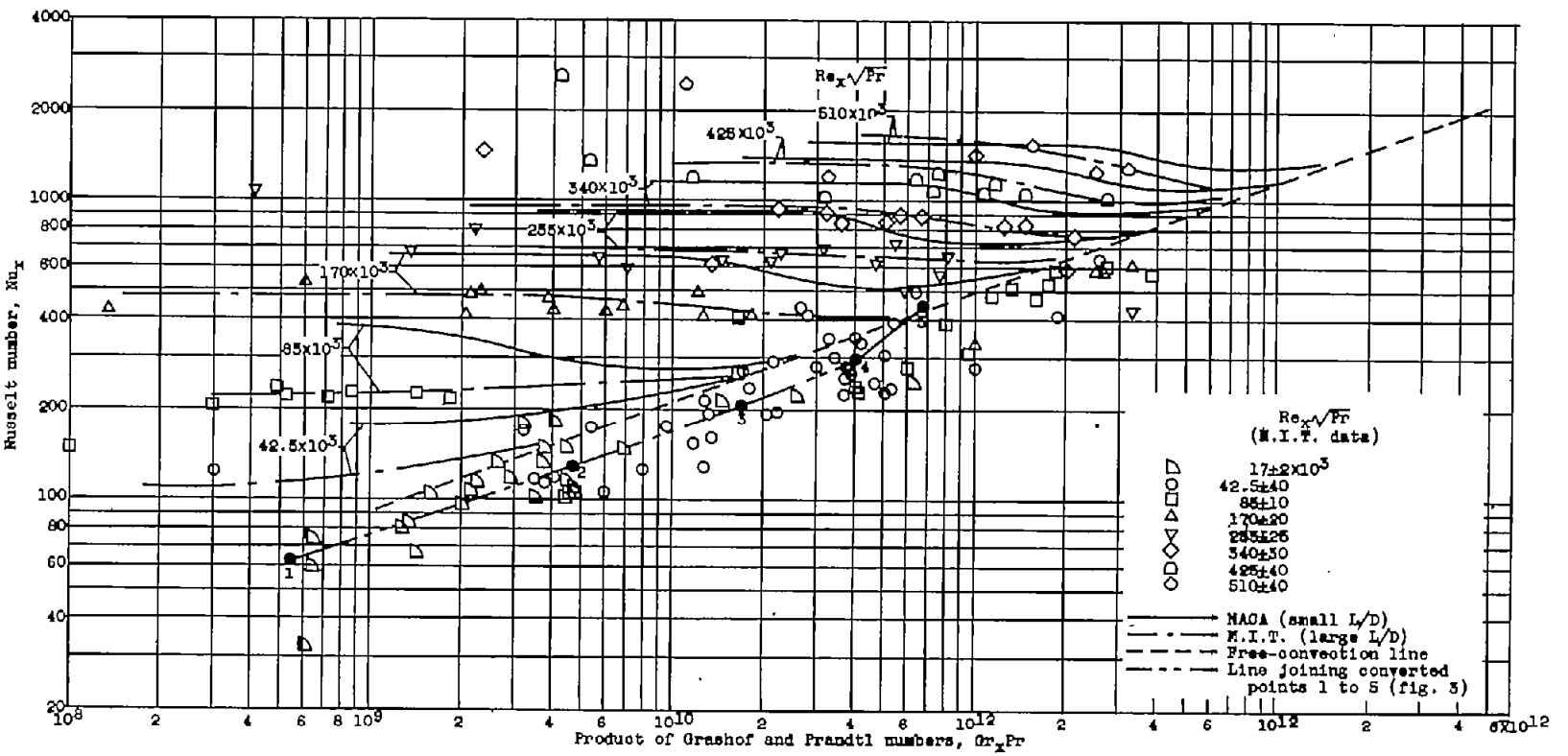

Figure 9. - Comparison of effects of free convection from correlations of heat-transfer data for tubes with small and large length-to-diameter ratios.

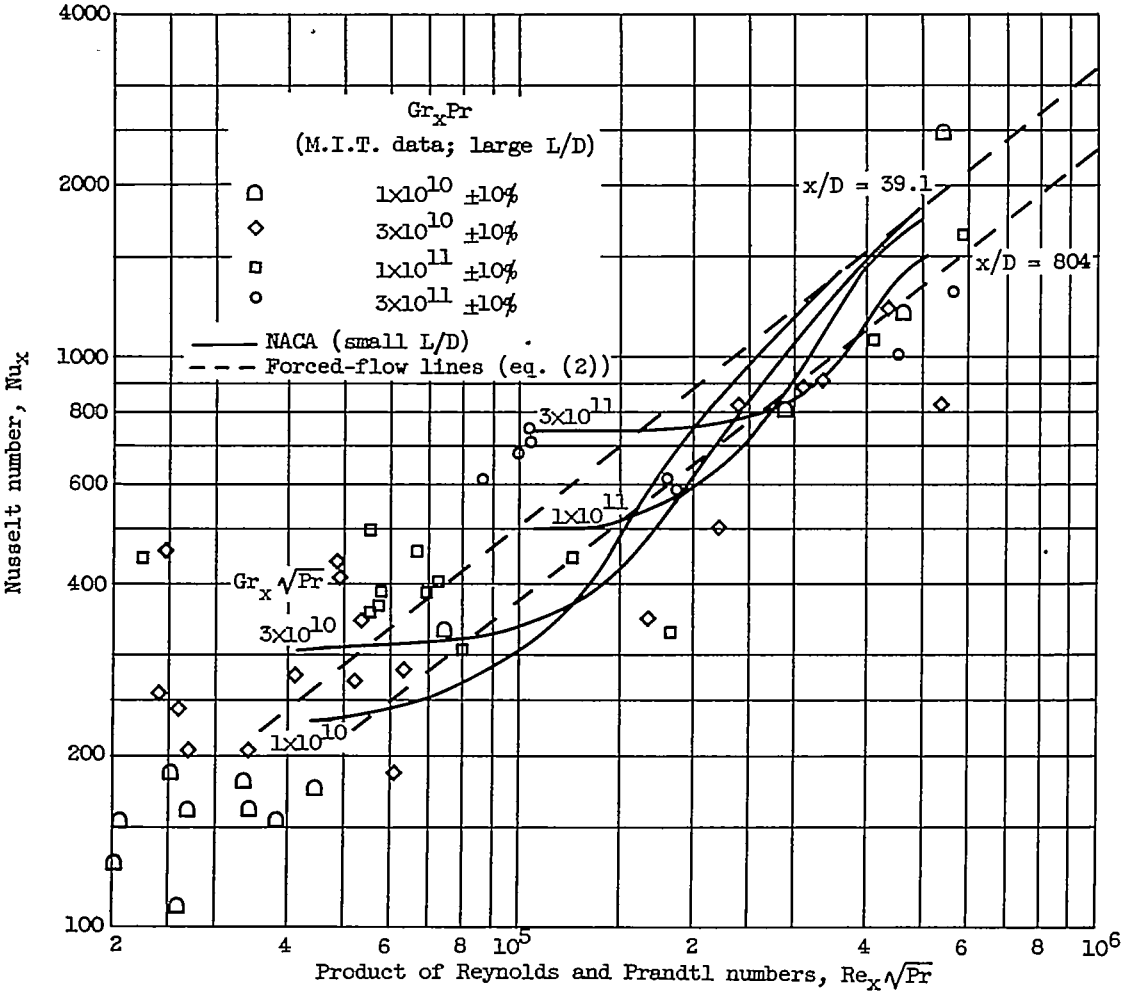

Figure 10. - Comparison of effects of forced convection from correlations of heat-transfer data for tubes with small and large length-to-diameter ratio.